J. Condensed Matter Nucl. Sci. 15 (2015) 305–313

Research Article

Progress in Development of Diamond-based Radiation Sensor for Use in LENR Experiments

Charles Weaver*, Mark Prelas, Haruetai Kasiwattanawut, Joongmoo Shim, Matthew Watermann, Cherian Joseph Mathai and Shubra Gangopadhyay

SKINR – University of Missouri, USA

Eric Lukosi

University of Tennessee, Knoxville, USA

Abstract

This work discusses the ongoing development of diamond-based radiation sensors for spectrometry within the environments found in low energy nuclear reaction (LENR) experiments. Specifically discussed are the efforts to demonstrate the robustness of palladium-electrode sensors. This includes fabrication methods, characterization and calibration techniques, and the results of deuterium gas loading trials which demonstrate performance throughout the entire test. The results are positive. One notable peak in the spectrometry results; additional trials are required to both determine the cause of this peak and determine which criteria.
 ISSN 2227-3123

Keywords: Charged particle spectroscopy, Diamond sensors, Radiation detection

1. Introduction

Efforts to perform spectroscopy on any neutrons or charged particles which may be produced by low energy nuclear reaction (LENR) phenomena have predominantly used CR-39 chips [1–4]. Although CR-39 has been demonstrated to be a useful spectroscopy method [5] with relatively low material costs, several of its attributes [6] have driven investigation into other detection methodologies. Most notably, the treatment and analysis of CR-39 is time-intensive and it is an integrating detector, which prohibits it from being used in real-time analysis. Conversely, conventional neutron spectroscopy methods which provide real-time analysis, such as scintillation detectors, are difficult to implement within the active LENR environment where they will have the highest detection efficiency. Therefore they cannot detect particles which may only transport over very short distances. The most popular neutron spectroscopy systems also require post processing techniques for n–γ discrimination due to their different sensitivities for different types of ionizing radiation.

*E-mail: weavercl@missouri.edu

 ISSN 2227-3123

The recent availability of large, electronic-grade, single-crystal diamonds (EGSCD) has generated a great amount of work in the creation of diamond-based radiation detectors. EGSCD-based detectors possess a number of advantages which makes them applicable to LENR systems. The mechanical robustness, inert chemistry, and radiation hardness of diamond allows its use within hostile environments. High charge-carrier mobility and charge collection efficiency near 100% allow diamond to be used in real-time spectroscopy while the 5.5 eV band gap of diamond provides an inherently low noise floor across a wide temperature range. Diamond also exhibits a linear response with increasing energy deposition and has demonstrated a resolution less than one percent for high energy particles [7]. What makes diamond particularly relevant for neutron spectroscopy is its low photon interaction cross-section, which removes the need for the n–γ discrimination techniques required by scintillator-based detectors.

In short, the use of a diamond-based neutron sensor, referred to as a diamond sensor (DS) throughout the rest of this paper, incorporates the advantages of traditional solid-state systems with the advantages of real-time signal analysis while avoiding the issues commonly associated with both. The most significant downside for diamond-based radiation sensors is cost; the number of manufacturers is currently small, but costs will come down as production methods improve and more vendors become available. The method of adapting a diamond sensor for LENR experiments was initially described at ICCF-17. It consists of tasks which can be divided into three categories: sensor fabrication, creating surface features, and achieving high deuterium gas loading.

Fabrication of a diamond-based detector which is sufficiently resistant to the deuterium environments in LENR experiments is the first step. Preliminary results presented at ICCF-17 [8] described attempts to produce ohmic contacts on a diamond plate using the reactive sputtering of diamond-like carbon (DLC). However these contacts did not survive exposure to deuterium, and additional attempts to produce in the interim continued to demonstrate poor adhesion. This required us to evaluate alternate materials and deposition methods. This paper presents the fabrication methods of additional diamond sensors and the results of evaluating those diamond sensors; the materials and deposition techniques used to create the contacts, $I - V$ characterization of the contacts, the calibration of the sensors, and the results of their exposure to deuterium.

Once the procedure for fabricating deuterium-resistant ohmic contacts is sufficiently reproducible we will then develop treatment methods to produce the surface structures believed to be necessary for the production of LENR phenomena. The theoretical basis of how these structures facilitate LENR phenomena has been explained in the literature [9]. After the requisite surface structures have been observed using SEM techniques, the final step is achieving high gas loading. The methods used to achieve high loading will be those which have previously claimed reproducible LENR phenomena [10].

2. Fabrication

The successful fabrication and operation of a diamond sensor depends on three components: the diamond substrate, the electrical contacts, and the associated electronics for signal analysis. Two electronic-grade diamond plates of dimension $3\times3\times0.5$ mm diamond plate were purchased from Element Six for use as diamond substrates. The plates showed no signs of crystal defects or band gap impurities when previously characterized using Raman spectroscopy and spectrophotometry. Before metallization, any persistent organic compounds, oxide layers, and residual metallic ions were removed from the diamond plate using the RCA clean procedure listed in Table 1; after each step the diamonds were rinsed with deionized water and placed in a deionized water bath while the solution used in the next step was prepared.

Once cleaned, a diamond substrate was placed within a mask. The mask consisted of two plates: one which held the diamond in place by centering it within a hole 3 mm in diameter; the second used a hole 2 mm in diameter centered over the diamond plate to permit deposition on a small region of the substrate. The masked substrate was then attached within the deposition chamber for contact deposition. The previous efforts to fabricate diamond sensors reported at

Table 1. Diamond plate cleaning procedure.

Step	Solution	Temp. (°C)	Time (min)
1	Aqua Regia	150	20
2	NH_4OH:H_2O_2:H_2O (1 : 1 : 1)	150	20
3	Piranha	150	20
4	H_2SO_4:HNO_3:$HClO_4$ (1 : 1 : 1)	150	30

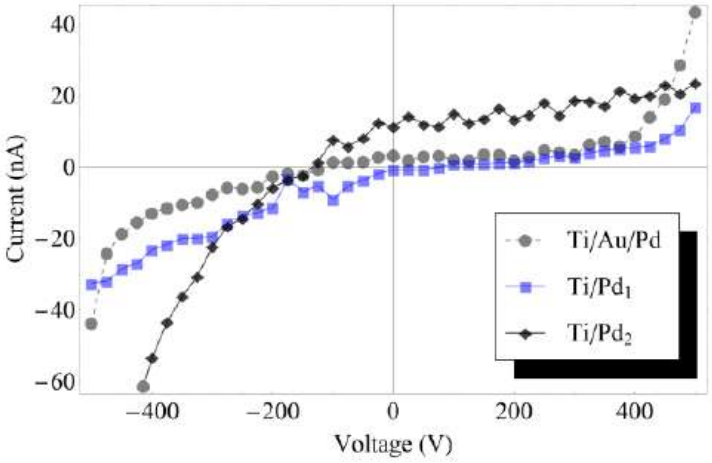

Figure 1. $I - V$ Characteristics of diamond sensors.

ICCF-17 used diamond-like carbon (DLC) films as the contact material; these contacts delaminated during deuterium loading and persistent difficulties with adhesion required the use of materials more commonly found in diamond contact formation: titanium, gold, and palladium. Titanium is one of the carbide-forming metals with a demonstrated history of producing ohmic contacts on diamond [11] but it requires oxygen and deuterium diffusion barriers. Without these barriers any titanium that exists in the contact, but is not bonded to the diamond, would react and damage the contacts. Palladium is used for two reasons: it is a lattice material metal which can achieve high loading and will therefore be treated to develop the microscale structures necessary for LENR to occur in future work; Pd is also an effective oxygen diffusion barrier. Gold was initially used as a deuterium diffusion barrier, but it was avoided in sensors 2 and 3 due to concerns regarding adhesion with the other materials. After one side of the diamond plate was metalized, the plate was removed from the mask, flipped over, replaced in the mask, and the same deposition process was performed on the other side.

Table 2. Diamond sensor film materials and thicknesses.

Sensor	Ti (nm)	Au (nm)	Pd (nm)
1	50	20	100
2	50	0	150
3	50	0	130

The film thicknesses deposited on the diamond plates are available in Table 2. The first of these diamond sensor fabrication attempts used three films which were all deposited by thermal evaporation: 50 nm base layer of titanium, 20 nm layer of gold, and 100 nm of palladium. During the Pu-239 calibration, discussed below, it became apparent that there was a problem with the contacts and the metalized plate was consequently inserted into an argon tube furnace for 20 min at 500˚C to promote the formation of TiC and improve contact quality. At some point during the annealing process the thin film delaminated from the diamond surface. These issues were avoided while constructing sensors 2 and 3 by replacing thermal evaporation with RF sputtering for titanium deposition. The gold layer was also removed and the palladium thickness was increased. The same film thicknesses were applied to both sides of a diamond plate; once one side had been metalized, the diamond was flipped over within the mask and the process was repeated.

3. Characterization and Calibration

Once both depositions were complete, a now-metalized diamond was mounted using silver paste onto a transistor package which featured two electrically isolated legs. After the silver paste dried, two wire bonds were made using aluminum wire 20 μm in diameter. One bond connected the package to the ground leg of the applied bias; the other bond connected the exposed palladium surface of the diamond sensor to the high voltage leg of the applied bias. The current–voltage characteristics of the assembled diamond sensor were then measured using a Keithley 6487 picoammeter. Each sensor exhibited the desired ohmic behavior between 150–250 V bias as shown in Fig. 1 which was previously determined to be the bias which achieved 100% charge collection efficiency for these sensors [8].

Each diamond sensor was then installed in a Canberra 7404 alpha spectrometer and energy-calibrated using a Pu-239 check source. The results of energy calibration are available in Fig. 2. The calibration curve of sensor 1, labeled TiAuPd, displays two peaks. The peak on the right corresponds to the expected full-energy peak of Pu-239 at 5156 keV. The peak below 2000 keV was the motivation for annealing and subsequent loss of the contact discussed above. The second sensor ($TiPd_1$) displays an unexpectedly high noise but was tested for deuterium resistance. The curve which corresponds to the third sensor, labeled $TiPd_2$, features the expected spectrum.

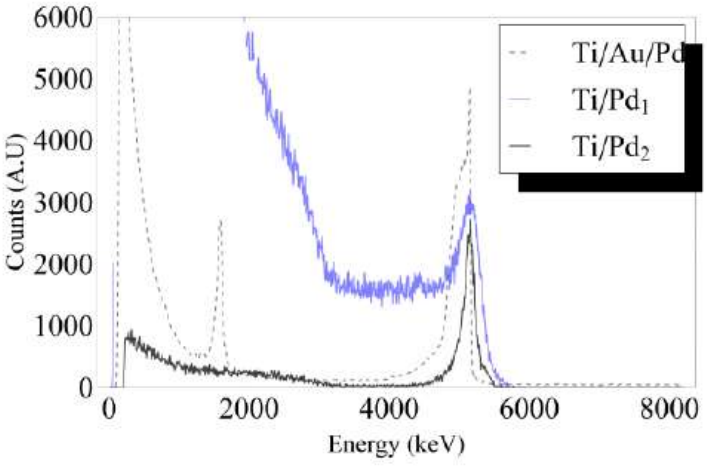

Figure 2. Pu-239 Diamond sensor energy calibration spectra.

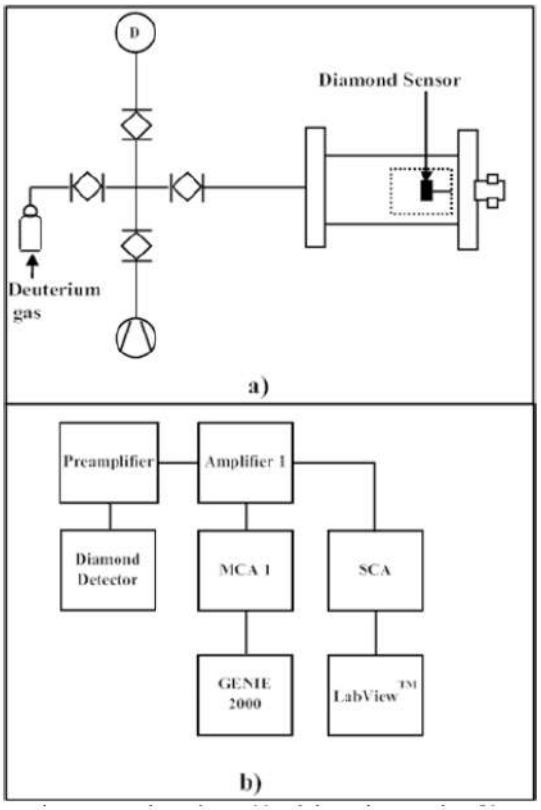

Figure 3. Experimental setup (a) and electronic connections (b).

4. Gas Loading Setup and Procedure

The diamond sensor under investigation was removed from the alpha spectrometer after calibration and connected within the chamber shown in Fig. 3a. The diamond sensor was then connected to the associated electronics shown in Fig. 3b by the BNC feedthrough on the chamber. The electronics for signal processing consisted of a preamplifier, two amplifiers, one single-channel analyzer, one card of a Canberra Multiport II USB Multichannel Analyzer array, and two independent computers which operated the Canberra Genie2000 spectroscopy and LabView edge-counting software programs.

Before initiating a gas trial, the chamber containing the diamond sensor was vacuumed using a roughing pump to a pressure below 13 Pa measured using an MKS 722 Baratron absolute capacitance manometer. After sufficient degassing of materials which had adhered to the inner surface of the chamber, a trial was initiated by closing the vacuum valve and opening the valve to the deuterium tank to fill the chamber with deuterium at a pressure of 690 kPa. A +200 V bias was then applied to the chip and both software programs were started simultaneously. To minimize the number of atmosphere changes for each sensor, trials were run as long as possible; the durations of the diamond sensor trials are shown in Table 3.

At the conclusion of each trial the chamber was opened and the diamond sensor was inspected using three methods.

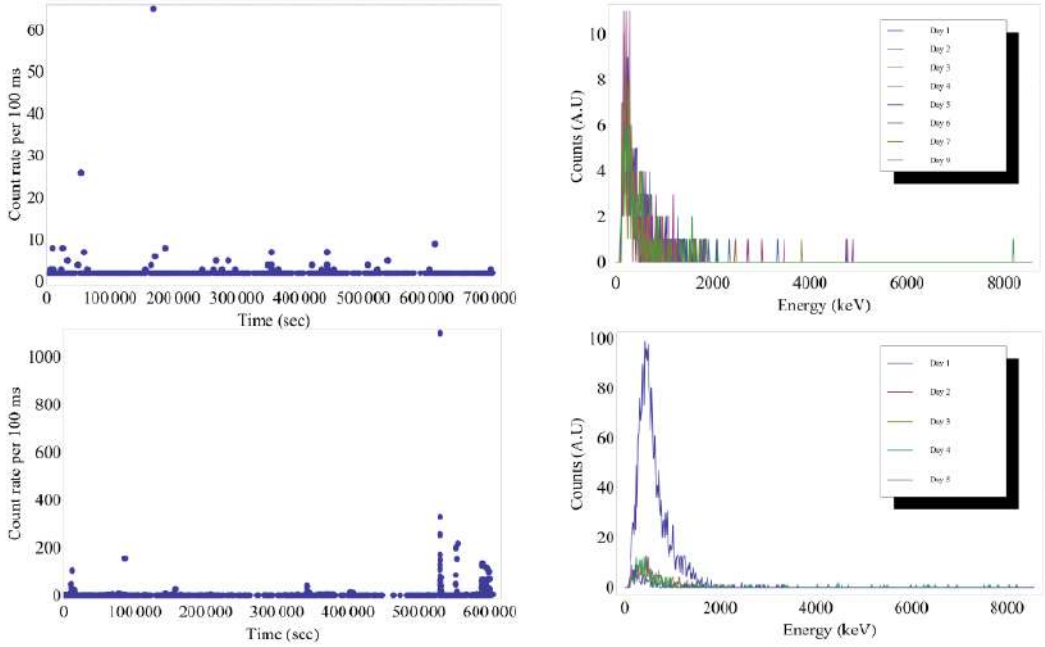

Figure 4. SCA (*left*) and spectroscopy (*right*) results for diamond sensor 2 – $TiPd_1$ trials 1 (*top*) and 2 (*bottom*).

Table 3. Diamond sensor trial durations.

Sensor	Trial	Duration (days)
2 – $TiPd_1$	2 – 1	9
2 – $TiPd_1$	2 – 2	5
3 – $TiPd_2$	3 – 1	7

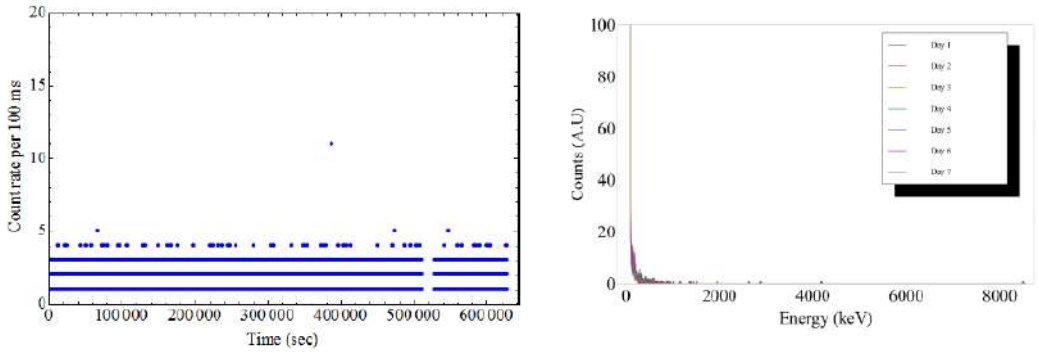

Figure 5. SCA (*left*) and spectroscopy (*right*) results for diamond sensor 3 – $TiPd_2$.

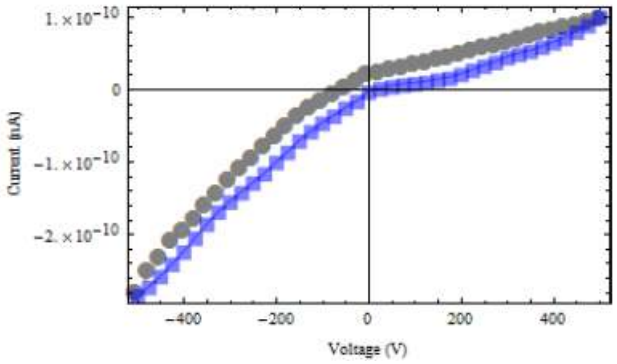

Figure 6. $I - V$ Characteristics of diamond sensor 2 after two deuterium loadings.

The energy calibration of the sensor was rechecked using the Pu-239 calibrated source. The detector $I - V$ behavior was rechecked to determine if any significant changes in the electrical behavior of the sensor took place during deuterium exposure. Scanning electron microscopy was used to locate any microscale defects which have been observed in the literature [12].

5. Results

The first diamond sensor (TiAuPd) failed during annealing. Diamond sensors 2 and 3 appear to have survived the deuterium exposure while producing some interesting results. The spectroscopy and counting results of deuterium exposure for diamond sensors 2 and 3 are available in Figs. 4 and 5, respectively. The spectroscopy results of trials 2 – 1 and 3 – 1 contain no peaks above the noise floor, although count rate data include rare occurrences of counts rates far above the background. Spectroscopy and count rate data also suggest that some reaction occurred with an average energy of 650 keV and FWHM of 400 keV on day five of trial 2-2.

SEM scans of the sensors which were taken after each sensor trial was finished contained one anomalous result shown in point of little evidence of the micro-ruptures or other irregular particle phenomena described in the literature

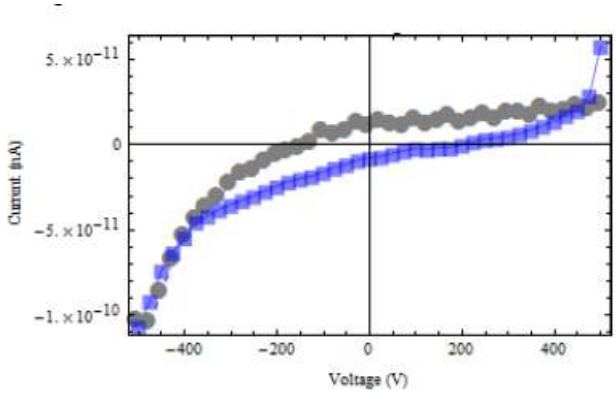

Figure 7. $I - V$ Characteristic of diamond sensor 3 after deuterium loading.

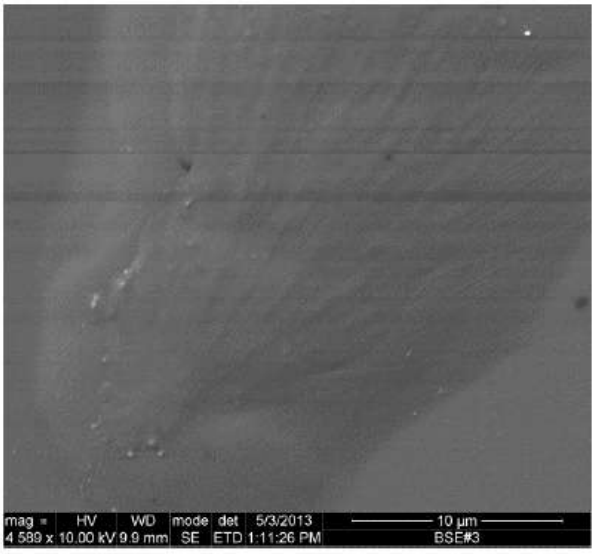

Figure 8. Anomalous spot found during SEM inspection of diamond sensor 2 after second deuterium loading.

[4]. The contact resistance of sensors 2 and 3 decreased during deuterium exposure which improved the $I - V$ curves shown in Figs. 6 and 7. Figure 6 shows $I - V$ Characteristics of diamond sensor 2 after two deuterium loadings and Fig. 7 shows $I - V$ Characteristic of diamond sensor 3 after deuterium loading.

6. Conclusions

The results of this work confirm progress in the development of diamond-based radiation sensors with the end goal of *in situ* incorporation for LENR experiments. It demonstrates diamond sensors which exhibit the same diagnostic responses before and after deuterium exposure which suggests that the sensor continue to function within the deuterium environment. Spectroscopy and counter data suggest that some reaction occurred within the cathode during deuterium pressure loading. However no conclusions can be made at this time regarding the source of these apparent energy peaks. They may have been the result of contact deformation as metallic titanium within the contacts absorbed deuterium which migrated through the outermost palladium film. Similarly, palladium is known to deform with deuterium loading and this may have also released the charge which was interpreted by the electronics to be an energetic particle.

This will be examined in the diamond sensors currently under development, which will reincorporate gold into the films as an intermediate to prohibit deuterium diffusion into the titanium. Once those sensors have demonstrated their resistance to deuterium, the exposed palladium electrode can be prepared using techniques in the literature to achieve the requisite microstructures. Once the surface preparation is sufficiently reproducible, the complete sensors can then be exposed to a high deuterium loading. Previously reported results can then be independently evaluated using real-time spectrometry which is effectively a part of the active nuclear environment.

Acknowledgements

The authors would like to thank the Sidney Kimmel Institute for Nuclear Renaissance at the University of Missouri for their scientific, administrative, and economic support personnel of this work.

References

[1] S. Mahadeva, Wide-ranging studies on the emission of neutrons and tritium by LENR configurations: an historical review of the early BARC results, *Low-Energy Nuclear Reactions and New Energy Technologies Sourcebook*, Volume 2, American Chemical Society, 2009, pp. 35–57.
[2] M.A. Prelas and E. Lukosi, Neutron emission from cryogenically cooled metals under thermal shock, *Proc. 17 th Int. Conf. on Cold Fusion*, Daejeon/Korea, 2012, pp. 13–17.
[3] S. Szpak, P. Mosier-Boss, F. Gordon, J. Dea, M. Miles, J. Khim and L. Forsley, LENR research using co-deposition, *Proc. ICCF14* (2008).
[4] P.A. Mosier-Boss, A review on nuclear products generated during low-energy nuclear reactions (LENR), *J. Condensed Matter Nucl. Sci.* **6** (2012) 135.
[5] J.A. Frenje, C.K. Li, F.H. Séguin, D.G. Hicks, S. Kurebayashi, R.D. Petrasso, S. Roberts, V.Y. Glebov, D.D. Meyerhofer, T.C. Sangster, J.M. Soures, C. Stoeckl, C. Chiritescu, G.J. Schmid and R.A. Lerche, Absolute measurements of neutron yields from DD and DT implosions at the OMEGA laser facility using CR-39 track detectors, *Rev. Sci. Instr.* **73** (2002) 2597.
[6] S.A. Durrani, Nuclear tracks today: Strengths, weaknesses, challenges, *Radiation Measurements* **43** (2008) S26–S33.
[7] C. Manfredotti, CVD diamond detectors for nuclear and dosimetric applications, *Diamond and Related Materials* **14** (2005) 531–540.
[8] E. Lukosi, M. Prelas, J. Shim, H. Kasiwattanawut, C. Weaver, C.J. Mathai and S. Gangopadhyay, Diamond-based radiation sensor for LENR experiments part 1: sensor development and characterization, *17th Int. Conf. Cold Fusion*, ICCF-17 Secretariat, Daejeon, Korea, 2012, p. 6.
[9] E. Storms, B. Scanlan, N. Santa Fe and C. Greenwich, Role of cluster formation in the LENR process, *15th Int. Conf. on Condensed Matter Nuclear Science*, 2009. Rome, Italy: ENEA. p, 2009.
[10] E. Storms, Status of cold fusion (2010), *Naturwissenschaften* **97** (2010) 861–881.
[11] T. Tachibana, B. Williams and J. Glass, Correlation of the electrical properties of metal contacts on diamond films with the chemical nature of the metal-diamond interface. II. Titanium contacts: A carbide-forming metal, *Phy. Rev. B* **45** (1992) 11975.
[12] M. Srinivasan, Neutron emission in bursts and hot spots: signature of micro-nuclear explosions? *J. Condensed Matter Nucl. Sci.* **4** (2011) 12.